



Contents lists available at ScienceDirect

## Bioorganic &amp; Medicinal Chemistry Letters

journal homepage: [www.elsevier.com/locate/bmcl](http://www.elsevier.com/locate/bmcl)

## Structure-based design of guanosine analogue inhibitors targeting GTP cyclohydrolase IB towards a new class of antibiotics

George N. Samaan<sup>a</sup>, Naduni Paranagama<sup>a</sup>, Ayesha Haque<sup>a</sup>, David A. Hecht<sup>b,c</sup>,  
Manal A. Swairjo<sup>a,\*</sup>, Byron W. Purse<sup>a,\*</sup>

<sup>a</sup> Department of Chemistry and Biochemistry and the Viral Information Institute, San Diego State University, San Diego, CA 92182, USA

<sup>b</sup> Department of Chemistry and Biochemistry, San Diego State University, San Diego, CA 92182, USA

<sup>c</sup> Department of Chemistry, Southwestern College, Chula Vista, CA 92120, USA

## ARTICLE INFO

**Keywords:**  
Antibiotic  
Resistance  
Folate  
GTP  
Nucleoside

## ABSTRACT

GTP cyclohydrolase (GTYH-I) is an enzyme in the folate biosynthesis pathway that has not been previously exploited as an antibiotic target, although several pathogens including *N. gonorrhoeae* use a form of the enzyme GTYH-IB that is structurally distinct from the human homologue GTYH-IA. A comparison of the crystal structures of GTYH-IA and -IB with the nM inhibitor 8-oxo-GTP bound shows that the active site of GTYH-IB is larger and differently shaped. Based on this structural information, we designed and synthesized a small set of 8-oxo-G derivatives with ether linkages at O<sup>6</sup> and O<sup>8</sup> expected to displace water molecules from the expanded active site of GTYH-IB. The most potent of these compounds, **G3**, is selective for GTYH-IB, supporting the premise that potent and selective inhibitors of GTYH-IB could constitute a new class of small molecule antibiotics.

Antibiotic resistance is a growing global health crisis, exacerbated by many factors.<sup>1</sup> The economics of antibiotic development are less favorable than those of drug development against chronic diseases and resistance to new antibiotics now typically emerges within two years of clinical approval, a result of horizontal transfer, high bacterial mutation rates, and the prevalence of antibiotic overuse and misuse.<sup>2</sup> For example, many cases of treatment failure with third generation cephalosporins, the final option of treatment for gonorrhoea, have been reported.<sup>3</sup> Therefore, to fight against the high resistance to antibiotics, novel classes of drugs with new mechanisms of action must be developed. Ongoing efforts by many academic and industrial labs continue to advance new antibiotic compounds towards the clinic, but as many recent reviews have highlighted, the vast majority of these compounds are synthetically modified derivatives of proven antibiotic scaffolds.<sup>1,2,4,5</sup>

The folate biosynthesis pathway is an established therapeutic target for antibiotics.<sup>6</sup> Drugs that block this pathway, specifically trimethoprim and sulfamethoxazole, are listed on the WHO's 2017 Model List of Essential Medicines. The trimethoprim-sulfamethoxazole combination is widely used as a first-line treatment for methicillin-resistant strains of *S. aureus*, but high levels of resistance to trimethoprim have emerged from a F98Y point mutation in prokaryotic dihydrofolate reductase (DHFR), its enzymatic target.<sup>7,8</sup> Sulfamethoxazole inhibits

dihydropteroate synthetase, an enzyme downstream of DHFR in the folate biosynthesis pathway. Inhibition of folate biosynthesis depletes this essential cofactor in prokaryotes, disrupting the synthesis of purines, thymidylate, pantothenate, glycine, serine, and methionine, and resulting in cell death.<sup>9</sup> Because of the clinical success of antifolate antibiotics and the emerging resistance to these drugs, we believe that a new class of antibiotics targeting an unexploited enzyme of folate biosynthesis, GTP cyclohydrolase IB, would present a prime opportunity to target resistant pathogens that rely on this enzyme.

GTP cyclohydrolase I (GTYH-I) is the first enzyme of the prokaryotic *de novo* biosynthetic pathway to folate (Fig. 1). It has been deemed an unsuitable drug target because prokaryotic GTYH-I and human GTYH-I, which catalyzes a step in the essential bioprotein biosynthesis pathway,<sup>10</sup> are highly homologous. In 2006, however, a prokaryote-specific type I GTP cyclohydrolase subfamily was discovered in a bioinformatic analysis that revealed the absence of the *folE* gene encoding the canonical GTYH-I in a number of clinically important pathogens, all of which possess the remaining genes for the folate biosynthesis pathway.<sup>11</sup> Further investigation showed that these microbes express an alternative GTYH-I enzyme that exhibits virtually no sequence homology to the canonical enzyme, yet carries out the same catalytic function.<sup>12</sup> The new enzyme is prokaryote-specific and was named GTYH-IB (and the corresponding gene *folE2*) while the canonical

\* Corresponding authors.

E-mail addresses: [mswairjo@sdsu.edu](mailto:mswairjo@sdsu.edu) (M.A. Swairjo), [bpurse@sdsu.edu](mailto:bpurse@sdsu.edu) (B.W. Purse).

<https://doi.org/10.1016/j.bmcl.2019.126818>

Received 15 October 2019; Received in revised form 7 November 2019; Accepted 8 November 2019

0960-894X/© 2019 Elsevier Ltd. All rights reserved.

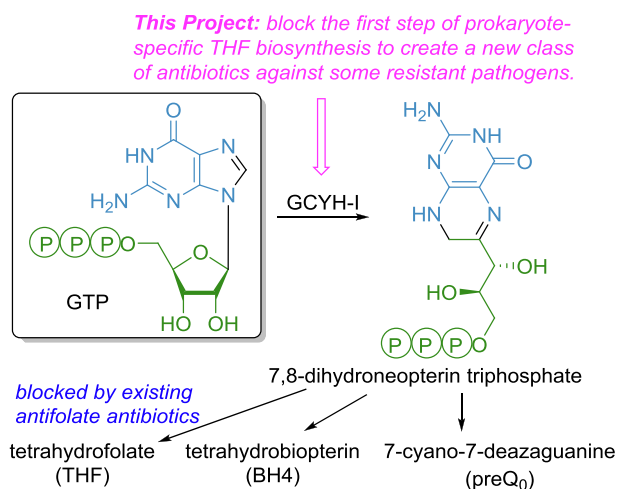


**Fig. 1.** Inhibition of prokaryote-specific GCYH-IB, the first enzyme in the *de novo* tetrahydrofolate (THF) biosynthesis pathway, is proposed for the creation of a new class of antifolate antibiotics.

enzyme was renamed GCYH-IA (and its gene *folE1*). GCYH-IB provides the sole enzymatic activity for the first step of folate biosynthesis in the clinically important pathogen genera *Staphylococcus* and *Neisseria*, making it an attractive and novel drug target.<sup>11</sup> Indeed *yciA*, the *S. aureus* gene encoding GCYH-IB, is an essential gene, and in bacteria that possess both the IA and IB enzymes, GCYH-IB, which uses Zn<sup>2+</sup> for catalysis, is essential in a  $\Delta folE$  background or when Zn<sup>2+</sup> is limiting.<sup>12,13</sup>

Both GCYH-IA and -IB catalyze the conversion of GTP to 7,8-dihydroneopterin triphosphate (H<sub>2</sub>NTP; Fig. 1), a multistep reaction that begins with addition of water to C8 of the guanine nucleobase, includes the elimination of formaldehyde, and leads to the incorporation of C1' and C2' of ribose into the 7,8-dihydroneopterin heterocycle following Amadori rearrangement.<sup>14-17</sup> 8-oxo-GTP binds strongly in the active site of GCYH-I but is not a substrate for this reaction because it displaces the nucleophilic water molecule from the active site and fills the vacated space with its C8-carbonyl group, which coordinates to the active site Zn<sup>2+</sup>.<sup>14-16,18,19</sup> Against *N. gonorrhoeae* GCYH-IB, 8-oxo-GTP is the most potent known inhibitor with  $K_i = 150$  nM, but this compound has a 28-fold lower  $K_i = 5.4$  nM against *T. thermophilus* GCYH-IA.<sup>14,15</sup> Crystallographic studies show that both GCYH-IA and -IB are members of the tunneling-fold (T-fold) structural superfamily, but the active sites are shaped significantly differently.<sup>12,14,15</sup> A comparison of the crystal structures of *N. gonorrhoeae* GCYH-IB and *T. thermophilus* GCYH-IA (the only available crystal structures of enzymes from each GCYH-I subfamily that contain bound 8-oxo-GTP) identifies three predominant regions of difference that could be exploited to improve inhibitor selectivity (Figs. 2, S1, and S2). The largest difference is in the region that we name Pocket 1 (size ~ 40 Å<sup>3</sup>), a site that is occupied by two water molecules when 8-oxo-GTP is bound to GCYH-IB.<sup>14</sup> This pocket is expected to be the easiest to address synthetically, because it projects directly outward from O<sup>6</sup> of the 8-oxoguanine nucleobase. Pocket 2 (size ~ 100 Å<sup>3</sup>) is predominantly above the plane of the nucleobase (as oriented in Fig. 2). Pocket 3 is the opening of the active site and accommodates the ribose and phosphate groups. The glycosidic bond angle is *anti* when 8-oxo-GTP is bound to GCYH-IA and *syn* in GCYH-IB, resulting in a substantially different conformation of the inhibitor.

Based on these crystallographically observed active-site differences, we propose that a new class of antifolate antibiotics can be developed by modifying the structure of 8-oxo-GTP so as to enhance potency against bacterial GCYH-IB and ablate binding to human GCYH-IA, which exhibits 45% overall sequence identity to *T. thermophilus* GCYH-IA (70% similarity) and identical active site residues and 3D structure (r.m.s.d. 0.86 Å over 817 C<sub>α</sub> atoms, see [supplementary Fig. S1](#)). We set

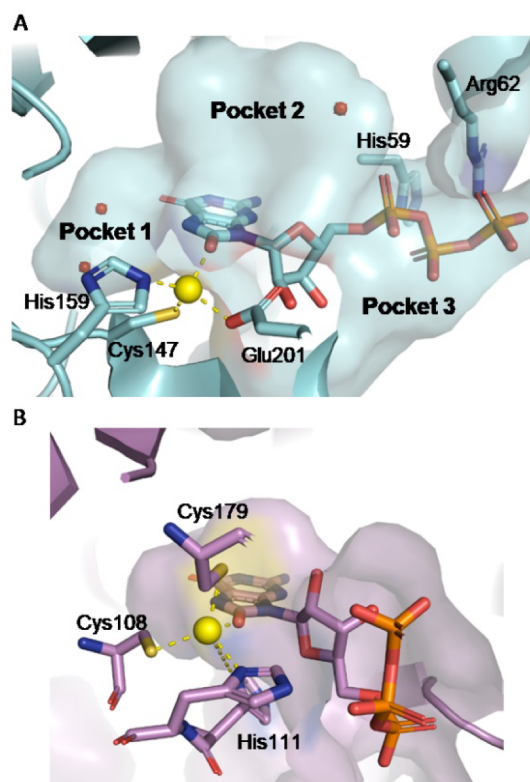


**Fig. 2.** Surface representations of the active site cavities of (A) *N. gonorrhoeae* GCYH-IB (PDB ID 5 K95),<sup>14</sup> and (B) *T. thermophilus* GCYH-IA (PDB ID 1WUQ),<sup>15</sup> both harboring bound 8-oxo-GTP and Zn<sup>2+</sup>, showing the additional space available in Pockets 1 and 2 of GCYH-IB. 8-oxo-GTP is shown in stick representation. The metal ion and water molecules are shown as yellow and red spheres, respectively. For additional representations of these cavities, see Figs. S1 and S2 in the Supplementary Data. (For interpretation of the references to colour in this figure legend, the reader is referred to the web version of this article.)

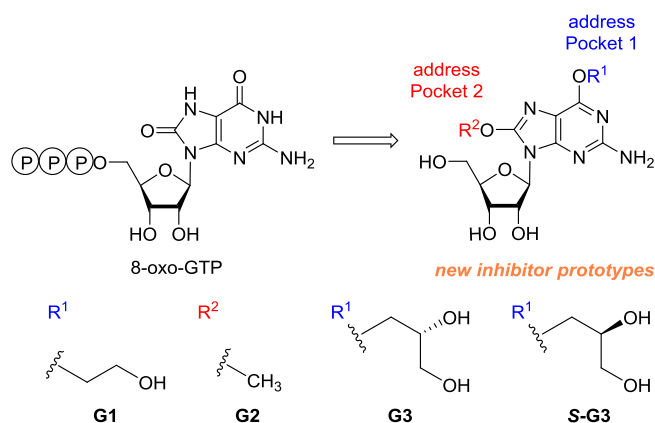
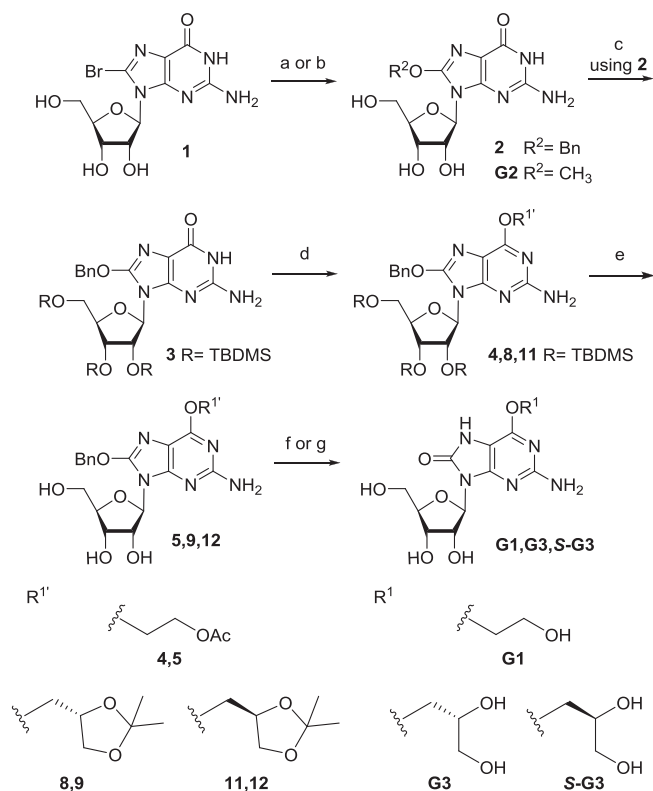


**Fig. 3.** Prototype inhibitor designs to probe the filling of Pockets 1 and 2 of GCYH-IB. For G1, G3, and S-G3, R<sup>2</sup> = H. For G2, R<sup>1</sup> = H.

out to design a small set of test compounds with increasingly large substituents oriented towards the larger active site pockets 1 and 2 of GCYH-IB (Fig. 3). To build up the inhibitor structure in the direction of Pocket 1, we envisioned modifying the enol tautomer at O<sup>6</sup> of 8-oxoguanine as a set of ethers decorated with alcohols to replace the hydrogen bonding interactions of the two water molecules that fill Pocket 1 when 8-oxo-GTP is bound. This enol ether design converts N1 from a protonated hydrogen bond donor to a hydrogen bond acceptor. Because of the position of N1 near Glu216, we anticipate that this change from



**Scheme 1.** Synthesis of nucleoside analogue inhibitors. Reagents and conditions: (a) sodium benzyloxide, DMSO, 65 °C, 16 h (65%) (to make 2); (b) sodium methoxide, DMSO, 50 °C, 16 h (39%) (to make G2); (c) TBDMSCl, imidazole, DMF, 50 °C, 5 h (65%); (d) (i) PPh<sub>3</sub>, dioxane, 80 °C, 45 min, 2-hydroxyethyl acetate (to make 4) or (S)-2,3-O-isopropylidene glycerol (to make 8) or (R)-2,3-O-isopropylidene glycerol (to make 11) (ii) DIAD, 60 °C, 2 h; (e) 1 M TBAF, THF, rt, 6 h (41% over 2 steps); (f) (i) 30% sodium methoxide in methanol, rt, 48 h, (ii) 2% HCl in methanol and H<sub>2</sub>O (61% for G1); (g) 2% HCl in methanol and H<sub>2</sub>O (61% for G3, 51% for S-G3).

donor to acceptor could be accommodated by a change in the protonation state of the neighboring glutamate (see below).

To synthesize the first compound G1, 8-bromoguanosine was used as the starting material (Scheme 1). Substitution of the bromine atom with a benzyloxy group was performed using freshly prepared sodium benzyloxide under conditions suitable for nucleophilic aromatic substitution (S<sub>N</sub>Ar). The resulting benzyl ether 2 was then allowed to react with *tert*-butyldimethylsilyl chloride (TBDMSCl) under basic conditions to protect the ribose hydroxyl groups, which would otherwise interfere with the Mitsunobu reaction. The protected nucleoside 3 was then treated with triphenylphosphine, diisopropylazodicarboxylate (DIAD) and 2-hydroxyethyl acetate under Mitsunobu conditions to give 4. Removal of the TBDMS groups was performed using tetrabutylammonium fluoride (TBAF) followed by removal of the acetyl and benzyloxy groups using basic and acidic conditions, respectively, to give the final product G1. G3 and its epimer S-G3 were synthesized using the same strategy as G1, using different substrates in the Mitsunobu reaction. Starting from the protected nucleoside 3, (S)- or (R)-2,3-O-isopropylidene glycerol was added to the reaction mixture along with PPh<sub>3</sub> and DIAD to give the acetal-protected Mitsunobu products 8 and 11, respectively. Treating 8 and 11 with TBAF and then aqueous acid provided the target compounds G3 and S-G3, respectively. For the synthesis of G2, 8-bromoguanosine was subjected to an S<sub>N</sub>Ar reaction using freshly prepared sodium methoxide to replace the bromine with a methoxy group, giving the final product G2.

With inhibitors G1–3 in hand, we measured their half-maximal inhibitory concentrations (IC<sub>50</sub>) *in vitro* against heterologously expressed

*N. gonorrhoeae* GCYH-IB (NgGCYH-IB) and a *H. sapiens* GCYH-IA (HsGCYH-IA) construct lacking the 42 N-terminal amino acids and previously reported to possess robust activity and improved solubility (for details on enzyme overexpression and purification, see the Supplementary Data).<sup>19</sup> Enzyme activity was measured using two previously established assays: an absorbance-based assay quantifying product H<sub>2</sub>NTP formation by its absorption at 330 nm; and a fluorescence-based assay that relies on post-reaction oxidation of the enzymatic product H<sub>2</sub>NTP to the fluorescent neopterin, and monitoring the neopterin emission peak at 446 nm with excitation at 365 nm (details of the assays are provided in the Supplementary Data).<sup>14</sup> First, steady-state kinetic analysis of HsGCYH-IA was performed using the fluorescence assay with GTP as substrate, and the analysis yielded a K<sub>M</sub> of 867 ± 57 μM (details are in Supplementary Data). Inhibition assays were then conducted by pre-incubating each enzyme with increasing concentrations of inhibitor compound (0–1600 μM) for 30 min, and measuring enzyme activity using the absorbance assay (for G1, G2 and S-G3) or the fluorescence assay (for G3), and a substrate concentration set at or near the enzyme's K<sub>M</sub> for GTP: 867 μM for HsGCYH-IA (this study), and 9 μM for NgGCYH-IB (experimental details are in the Supplementary Data; see also Fig. S3).<sup>14</sup> All enzymatic assays were performed in triplicate.

IC<sub>50</sub> values obtained from the inhibition data show that G1 has modest selectivity for HsGCYH-IA, G2 is not selective, and both G3 compounds are modestly selective for NgGCYH-IB, with G3 showing the greater selectivity (Table 1). G3 is three-fold more potent against NgGCYH-IB, a 31-fold reversal of selectivity as compared with our starting point, 8-oxo-GTP. Previous work shows that 8-oxo-GTP is 28-fold more potent against GCYH-IA from *T. thermophilus*, which harbors a nearly identical active site to HsGCYH-IA in sequence and 3D structure.<sup>14,15</sup> While these IC<sub>50</sub> measurements are indicative of only modest potency, the 31-fold reversal of selectivity in favor of the bacterial enzyme is significant and supports our structure-guided hypothesis on inhibitor optimization. We note also that G1–3 lack the phosphate groups of 8-oxo-GTP, which engage in ion pairing with arginine and lysine residues of the enzyme, leading to the phosphorylated inhibitor's sub-μM affinity.<sup>14</sup> Introducing one or more phosphate groups, or a suitable phosphate surrogate, in a future round of inhibitor refinement is expected to enhance the potency of G3 and related, future derivatives.

*In silico* docking studies were performed in which we docked 8-oxo-GTP and G3 into the GTP binding sites of the x-ray crystal structures of NgGCYH-IB (PDB ID 5K95),<sup>14</sup> and HsGCYH-IA (PDB ID 1FB1).<sup>19</sup> For the binding of G3, we performed docking both with and without the carboxylate of Glu216 protonated, and found a significantly better fit of G3 with the side chain protonated. This protonation change is predicted to accommodate the change of G3's N1 from hydrogen bond donor to acceptor in the course of synthesizing its enol ether appendage. The bound poses of 8-oxo-GTP docked into NgGCYH-IB as well as HsGCYH-IA are consistent with the inhibitor's crystallographically observed mode of binding to NgGCYH-IB. Likewise, the conformation of the pose of G3 docked into the active site of NgGCYH-IB is consistent with that of 8-oxo-GTP as seen bound in the crystal structure to NgGCYH-IB (Fig. 4).

**Table 1**

Measured half maximal inhibitory concentrations (IC<sub>50</sub>) of designed inhibitors against HsGCYH-IA and NgGCYH-IB. Values are presented with respect to their standard errors.

Inhibitor	IC <sub>50</sub> (μM)	
	HsGCYH-IA	NgGCYH-IB
G1	221 ± 10	413 ± 6
G2	514 ± 32	372 ± 25
S-G3	372 ± 14	164 ± 11
G3	409 ± 21	134 ± 11

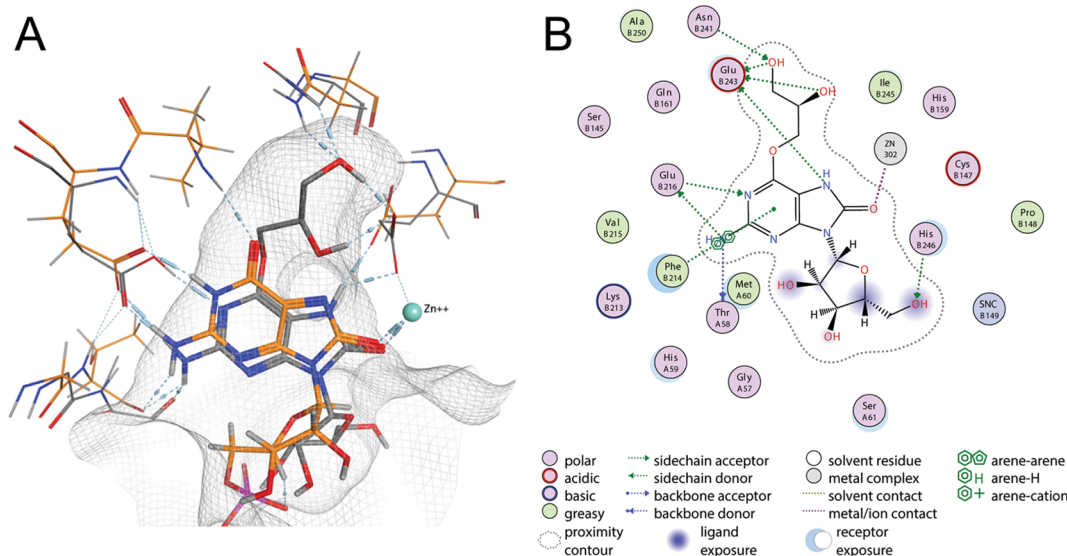


**Fig. 4.** A Bound pose of G3 (carbon in gray) superimposed on 8-oxo-GTP (carbon in orange) as seen bound in the active site in the crystal structure of NgGCYH-IB (5 K95). B Key protein-ligand interactions between the bound pose of G3 and NgGCYH-IB. (For interpretation of the references to colour in this figure legend, the reader is referred to the web version of this article.)

However, because of steric clashes in Pocket 1 with Q182, H210 and L165, we were not able to obtain a bound pose of G3 in HsGCYH-IA. These molecular modeling studies support the preferential inhibition of NgGCYH-IB by G3 on the grounds that its projections into Pocket 1 are too large to be accommodated by HsGCYH-IA.

GCYH-IB is a prokaryotic enzyme in the folate biosynthesis pathway that is essential for the proliferation of some pathogens, including *Staphylococcus* and *Neisseria*. Based on the architecture of its active site in comparison with the human orthologue GCYH-IA, we identified two active site regions, Pockets 1 and 2, that are larger and geometrically distinct in GCYH-IB. The use of a novel synthetic route allowed for the preparation of a small set of four 8-oxo-G analogue inhibitors that build into these active site pockets. Two of the analogues, G3 and S-G3, invert the selectivity of the parent inhibitor 8-oxo-GTP by up to 31-fold in the case of G3, now providing three-fold greater potency against NgGCYH-IB as compared with the human enzyme. Docking studies support the structure-based rationale for the inhibitor design and the observed change in selectivity for the bacterial enzyme. The glycerol ether of G3 projects into Pocket 1 where it is accommodated, but its bulk reduces compatibility and potency against the human enzyme. While these new inhibitors are not potent enough to be drug leads, their structure-guided design and the observation of the predicted change in selectivity to target the bacterial enzyme supports our premise that GCYH-IB can be exploited as a target for a new class of antibiotics.

#### Declaration of Competing Interest

The authors declare that they have no known competing financial interests or personal relationships that could have appeared to influence the work reported in this paper.

#### Acknowledgments

Financial support for this research was provided by San Diego State University; the National Institutes of Health [GM110588 to M.A.S.]; and the California Metabolic Research Foundation.

#### Appendix A. Supplementary data

Supplementary data to this article, including supplementary figures, general experimental information, synthetic procedures and compound

characterization data, enzyme expression and assay descriptions, and methods for docking studies, is available online at <https://doi.org/10.1016/j.bmcl.2019.126818>.

#### References

- Friedman D, Alper J. *Technological Challenges in Antibiotic Discovery and Development: A Workshop Summary*. Washington, DC: The National Academies Press; 2014. <https://doi.org/10.17226/18616>.
- Fischbach MA, Walsh CT. Antibiotics for emerging pathogens. *Science*. 2009;325:1089–1093. <https://doi.org/10.1126/science.1176667>.
- Gelband H, Miller-Petrie M, Pant S, et al. *The State of the World's Antibiotics*. Washington, D.C: CDDEP; 2015.
- Blair JMA, Webber MA, Baylay AJ, Ogbolu DO, Piddock LJV. Molecular mechanisms of antibiotic resistance. *Nat Rev Microbiol*. 2014;13:42. <https://doi.org/10.1038/nrmicro3380>.
- Hofer U. The cost of antimicrobial resistance. *Nat Rev Microbiol*. 2019;17:3. <https://doi.org/10.1038/s41579-018-0125-x>.
- Bourne CR. Utility of the biosynthetic folate pathway for targets in antimicrobial discovery. *Antibiotics*. 2014;3:1–28. <https://doi.org/10.3390/antibiotics3010001>.
- Dale GE, Broger C, D'Arcy A, et al. A single amino acid substitution in *Staphylococcus aureus* dihydrofolate reductase determines trimethoprim resistance 1. Edited by T. Richmond. *J Mol Biol*. 1997;266(1):23–30. doi:10.1006/jmbi.1996.0770.
- Heaslet H, Harris M, Fahnoe K, et al. Structural comparison of chromosomal and exogenous dihydrofolate reductase from *Staphylococcus aureus* in complex with the potent inhibitor trimethoprim. *Proteins Struct Funct Bioinforma*. 2009;76:706–717. <https://doi.org/10.1002/prot.22383>.
- Scocchera E, Wright DL. The Antifolates. In: Fisher JF, Mobashery S, Miller MJ, eds. Cham: Springer International Publishing; 2018:123–149. doi:10.1007/7355\_2017\_16.
- Thöny B, Auerbach G, Blau N. Tetrahydrobiopterin biosynthesis, regeneration and functions. *Biochem J*. 2000;347:1–16. <https://doi.org/10.1042/bj3470001>.
- El Yacoubi B, Bonnett S, Anderson JN, Swairjo MA, Iwata-Reuyl D, De Crécy-Lagard V. Discovery of a new prokaryotic type I GTP cyclohydrolase family. *J Biol Chem*. 2006;281:37586–37593. <https://doi.org/10.1074/jbc.M607114200>.
- Sankaran B, Bonnett SA, Shah K, et al. Zinc-independent folate biosynthesis: Genetic, biochemical, and structural investigations reveal new metal dependence for GTP cyclohydrolase IB. *J Bacteriol*. 2009;191:6936–6949. <https://doi.org/10.1128/JB.00287-09>.
- Chaudhuri RR, Allen AG, Owen PJ, et al. Comprehensive identification of essential *Staphylococcus aureus* genes using Transposon-Mediated Differential Hybridisation (TMDH). *BMC Genomics*. 2009;10:291. <https://doi.org/10.1186/1471-2164-10-291>.
- Paranagama N, Bonnett SA, Alvarez J, et al. Mechanism and catalytic strategy of the prokaryotic-specific GTP cyclohydrolase-IB. *Biochem J*. 2017;474:1017–1039. <https://doi.org/10.1042/BCJ20161025>.
- Tanaka Y, Nakagawa N, Kuramitsu S, Yokoyama S, Masui R. Novel reaction mechanism of GTP cyclohydrolase I. High-resolution X-ray crystallography of thermophilus HB8 enzyme complexed with a transition state analogue, the 8-oxoguanine derivative. *J Biochem*. 2005;138:263–275. <https://doi.org/10.1093/jb/mvi120>.
- Narp H, Huber R, Auerbach G, et al. Active site topology and reaction mechanism of GTP cyclohydrolase I. *Proc Natl Acad Sci U S A*. 1995;92:12120–12125. <https://doi.org/10.1073/pnas.92.26.12120>.

17. Yaylayan VA, Huyghues-Despointes A, Feather MS. Chemistry of Amadori rearrangement products: analysis, synthesis, kinetics, reactions, and spectroscopic properties. *Crit Rev Food Sci Nutr.* 1994;34:321–369. <https://doi.org/10.1080/10408399409527667>.
18. Wolf WA, Brown G. The biosynthesis of folic acid. X. Evidence for an Amadori rearrangement in the enzymatic formation of dihydroneopterin triphosphate from GTP. *Biochim Biophys Acta.* 1969;192:468–478. [https://doi.org/10.1016/0304-4165\(69\)90396-1](https://doi.org/10.1016/0304-4165(69)90396-1).
19. Auerbach G, Herrmann A, Bracher A, et al. Zinc plays a key role in human and bacterial GTP cyclohydrolase I. *Proc Natl Acad Sci.* 2000;97:13567–13572. <https://doi.org/10.1073/pnas.240463497>.